Environ Monit Assess (2022) 194: 644
https://doi.org/10.1007/s10661-022-10318-y

Modeling wildfire risk in western Iran based on the integration of AHP and GIS

Vahid Nasiri · Seyed Mohammad Moein Sadeghi · Rasoul Bagherabadi · Fardin Moradi · Azade Deljouei · Stelian Alexandru Borz

Received: 26 March 2022 / Accepted: 25 July 2022 / Published online: 5 August 2022

Abstract This study aimed at delineating the wildfire risk zones in a fire-prone region located in a rarely addressed area of western Iran (Paveh city) by assessing the potential of factors such as NDVI, topographic factors (elevation, slope, and aspect), land cover, and evaporation in explaining the fire occurrence probability. Analytic hierarchy process (AHP) and geographical information system (GIS) methods were used synergistically to integrate the mentioned factors into analysis, following an informed categorization of each factor based on the information on previous fire occurrence. In the AHP process, elevation and evaporation data were considered to be the most critical factors. It was found that the predicted wildfire risk areas were in agreement with past fire events by the use of the methodology proposed by this study. Accordingly, the study's final wildfire risk map indicated that approximately 64.7% of the study area is located in the high- and very high-risk zones. Land-use planners and decision-makers may use the developed map to setup and implement fire prevention strategies and enhance or develop the fire-surveillance logistics and infrastructure, including but not limited to the positions of fire watchtowers, fire lines, and fire sensors, with the aim to minimize potential fire impacts.

Keywords Analytic hierarchy process · Geographical information systems · Wildfire management · Wildfire risk · Zagros vegetation zone

V. Nasiri
Faculty of Civil Engineering, Transilvania University of Brasov, Brasov 900152, Romania

S. M. M. Sadeghi (✉) · A. Deljouei · S. A. Borz
Department of Forest Engineering, Forest Management Planning and Terrestrial Measurements, Faculty of Silviculture and Forest Engineering, Transilvania University of Brasov, Brasov 500123, Romania
e-mail: seyed.sadeghi@unitbv.ro; s.sadeghi@ufl.edu

S. M. M. Sadeghi · A. Deljouei
School of Forest, Fisheries and Geomatics Sciences, University of Florida, Gainesville, FL 32611, USA

R. Bagherabadi
Department of Environmental Sciences, Faculty of Natural Resources, University of Tehran, Karaj 1417643184, Iran

F. Moradi
Aerial Monitoring Research Group, Razi University, Kermanshah 6714414971, Iran

Introduction

Wildfire is among the most critical forest disturbances, having a high impact on greenhouse gas emissions (McGlynn et al., 2022), air pollution (Zhu et al., 2018), and climate change (Boucher et al., 2020). It also has a significant impact on forest regeneration (Santoro et al., 2021; Swan et al., 2021), wildlife, and habitat resilience (Sweitzer et al., 2016) and invariably causes high-level socio-economic losses (Nyamadzawo et al., 2013). In the past decade, much scientific attention has been given to identifying fire-driving factors (Naderpour et al., 2021;

Ozenen Kavlak et al., 2021), wildfire risk assessment (Liu et al., 2021; Nuthammachot & Stratoulias, 2021), and wildfire modeling (Emmett et al., 2021; Tiwari et al., 2021). To this end, wildfire risk (WR) is defined as the likelihood of fire to occur based on the nature and incidence of causative agents (Hardy, 2005). In recent years, many WR assessment studies have produced increasingly accurate wildfire risk indexes (WRI). WRI models use a wide range of fire-driving factors, remotely sensed data sets, spatial analysis techniques, and modeling approaches. For example, Novkovic et al. (2021) assessed WR in northwest Spain and produced a forest WRI map by the use of the Normalized Difference Vegetation Index (NDVI; from Sentinel-2), aerial LiDAR data, a high-resolution digital elevation model, vegetation layers, and analytic hierarchy processes (AHP) GIS-based spatial analysis. Their resulting maps showed that half of the study area was located in a high fire-risk zone. Most of the studies on the topic included a wide range of factors such as topography (Ma et al., 2020), land cover (Pham et al., 2020), temperature, evaporation, evapotranspiration (Sevinc et al., 2020; Ying et al., 2018), communication infrastructure, and human activities (Carrasco et al., 2021; Kim et al., 2019); these potential drivers were typically used to increase the model performance and reduce WR assessment uncertainties. Zhao et al. (2021) used topographic factors, temperature, NDVI, road distance, and distance to residential centers and produced a WRI map with an accuracy of 76.7%. In another study, Milanović et al. (2021) used in their WR model vegetation type, population density, topographic factors, and distance-based layers, including distance to roads and rails and arable and agricultural lands. All these studies agree that monitoring and modeling wildfires are complex processes because they involve factors playing various roles in different regions. That is why most studies planned their research on a local or regional scale (Eslami et al., 2021; Gigović et al., 2019; Satir et al., 2016) and it may be helpful to conduct WR assessments in different regions and produce regional-based WRI models to account for the variability in factors and scales.

Freely available remote sensing data such as the MODIS Fire Information for Resource Management System (FIRMS), Landsat, and the European Space Agency (ESA) Sentinel datasets were used as excellent sources to identify fire hot spots (Banerjee, 2021; Landi et al., 2021); calculate land surface temperature (Esfandeh et al., 2021), evapotranspiration (Roche et al., 2018), and vegetation indices (Ma et al., 2018; Moradi et al., 2022; Talucci et al., 2020); and also to develop land use and land cover maps (Nasiri et al., 2022; Sobhani et al., 2021). For mapping and further analyzing these datasets, GIS-based spatial analysis techniques have been used as powerful tools (Novkovic et al., 2021). Following the preparation of the datasets, approaches for reliable modeling of WR are required. For doing so, different modeling approaches such as machine learning models (Bot & Borges, 2022; Li et al., 2022), fuzzy models (Nebot & Mugica, 2021), and AHP (Nikhil et al., 2021) were used. As a multi-criteria decision analysis, AHP integrates easily with GIS and provides a clear, user-friendly, and straightforward modeling approach (Saaty, 1988). It is a powerful and flexible decision-making method used to rank different features (Coban & Erdin, 2020).

Wildfires are among the most critical problems in the Mediterranean and semiarid climate zones, affecting countries such as France (Ruffault & Mouillot, 2017), Spain (Quintano et al., 2018), Portugal (Carmo et al., 2011), Italy (Elia et al., 2020), Greece (Mallinis et al., 2018), Lebanon (Mitri et al., 2015), Turkey (Akbulak et al., 2018), and Iran (Bashari et al., 2016; Jaafari et al., 2017). In Iran, each year, the Zagros Mountainous vegetation zone having a Mediterranean and semiarid climate experiences pasture fires that affect the sparse forest resources and cause irreparable damage to the region's ecosystems. High regional fire frequency and the lack of quality information have guided this study to assess the WRs and determine the high-risk areas in these valuable ecosystems. Hence, this study aimed at generating a WR map for the fire-prone part of the Mediterranean region of Iran. This was achieved through the application of AHP and GIS tools to analyze the relationship between potential factors and the risk of wildfire.

Materials and methods

Study site

The study site is located in the Zagros Mountains vegetation zone, west of Iran (Paveh city). The study area holds approximately 80,514 ha and extends between latitudes 35° 01′–35° 04′ N and longitudes 46° 20′–46° 23′ E (Fig. 1), with the mean elevation of 1540 m above sea level. The area has been largely affected

by wildfire events, with the highest WR occurring during the dry season (i.e., May to September). The annual precipitation varies between 600 and 800 mm and the minimum rainfall occurs in the middle of summer. In the studied region, dominant tree species include Persian oak (*Quercus brantii*), gall oak (*Q. infectoria*), wild pistachio (*Pistacia atlantica*), and Montpellier maple (*Acer monspessulanum*).

Overall methodology

This study considered all the available factors that can affect wildfire occurrence. To assess the risk of wildfire, several sources of information were used, including satellite imagery, land cover maps, climatic data, and topographic features. All the layers were mapped and resampled at a 10-m resolution using the bilinear interpolation method (e.g., Jiang et al., 2021; Lanaras et al., 2018). After that, we classified each layer based on previous wildfire information into four classes: low, moderate, high, and very high WR levels. Finally, a WR map was produced based on the AHP- and GIS-based map algebra. Figure 2 illustrates the workflow we used to construct the WR model.

Wildfire risk (WR) factors

This study involved all the available factors in the modeling workflow and producing an accurate WRI map. We extracted a high-resolution vegetation index from satellite images as the starting point for wildfire factors preparation. The vegetation index is used to account for the vegetation density as an attribute in WRI model construction. Based on previous studies, NDVI can provide valuable information about the health status of trees, moisture content, and productivity (Amiri & Pourghasemi, 2022; Jiang et al., 2022). In this regard, the Level-1C products of Sentinel-2A (S-2A), a multispectral instrument covering 13 spectral bands (443–2190 nm), with a swath width of 290 km and a spatial resolution of 10 m (four visible and near-infrared bands), 20 m (six red edge and shortwave infrared bands), and 60 m (three atmospheric correction bands), dated 2019–08-11, were downloaded from the Copernicus Open Access Hub (https://scihub.copernicus.eu/) and corrected atmospherically using Sen2Cor (Ver. 2.5.5). Sen2Cor converts the top of atmosphere reflectance (TOA) to the bottom of atmosphere reflectance (BOA) and generates Level-2A products. Then we used band 4 (665 nm, 10 m spatial resolution) and band 8 (842 nm, 10 m

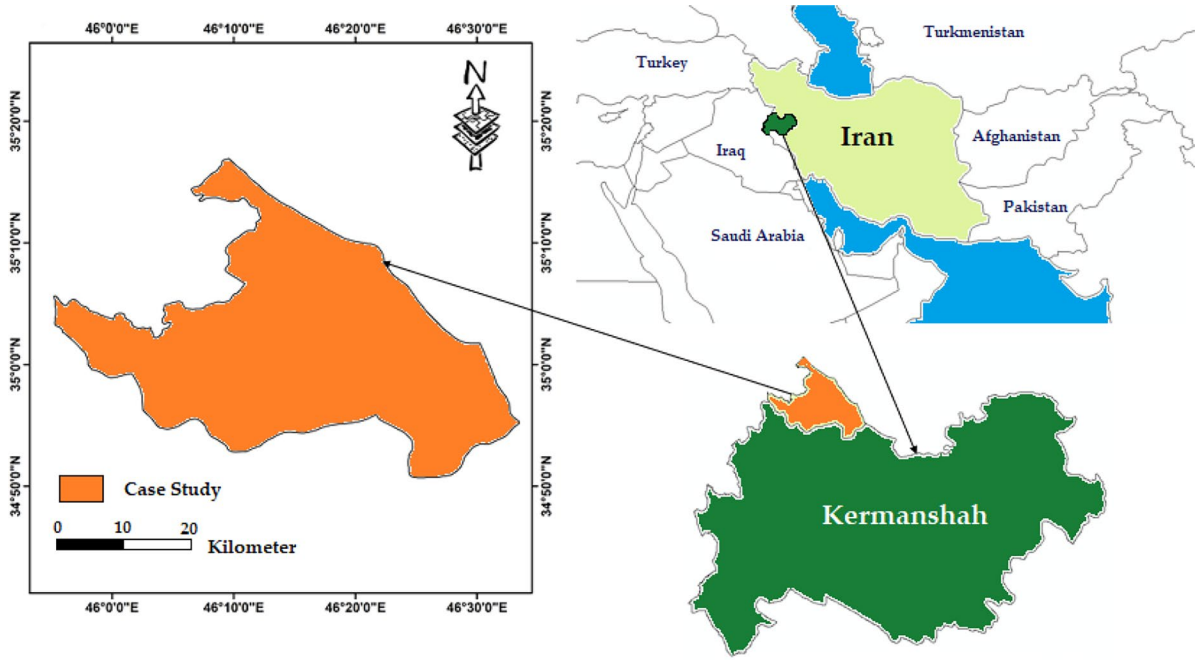

Fig. 1 The geographic location of study area

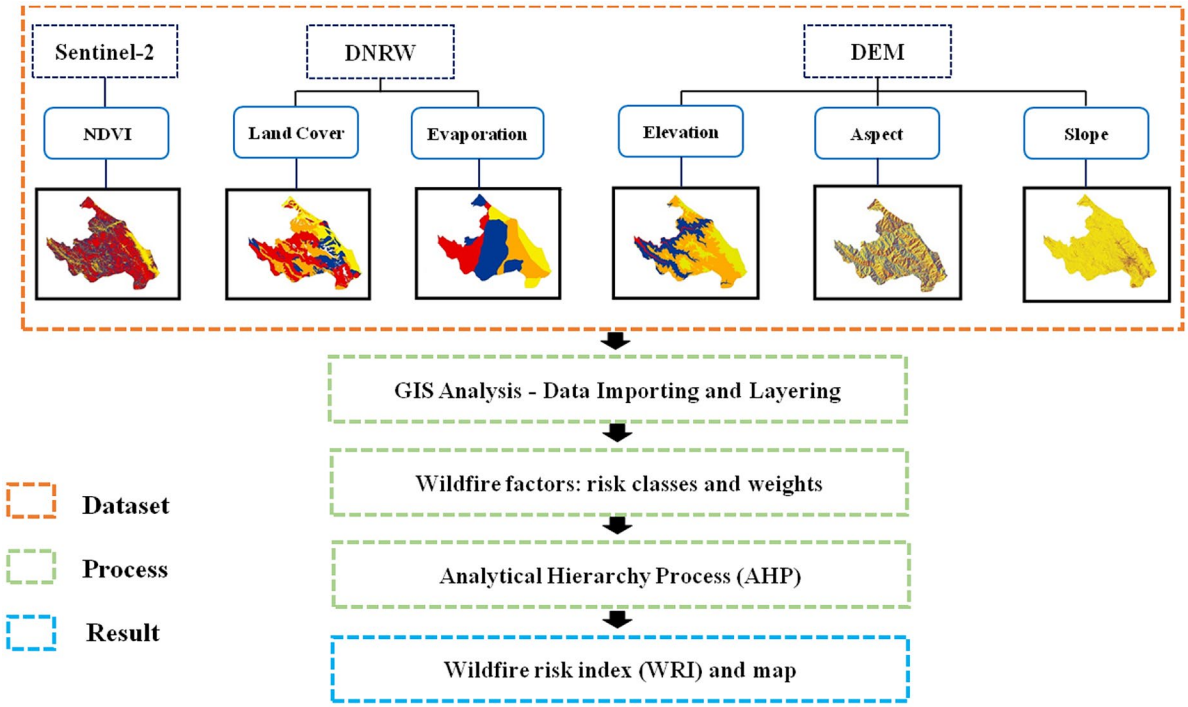

Fig. 2 Workflow of wildfire risk (WR) model construction, which consists of datasets, data processing, and results

spatial resolution) to extract the NDVI based on Eq. 1. The analysis was implemented in the SNAP (Ver. 8.0.5) software.

$$NDVI = \frac{Band8 - Band4}{Band8 + Band4} \quad (1)$$

Also, previous studies reported that topographic factors such as elevation, slope, and aspect could influence the probability of fire occurrence (Airey-Lauvaux et al., 2022; Si et al., 2022). This information can be extracted from high-resolution Digital Elevation Models (DEM). We used the ALOS PALSAR—Radiometric Terrain Correction (resolution 12.5 m) DEM (https://asf.alaska.edu). Slope and aspect layers were produced by extracting the elevation from the DEM layer. Data related to land cover and evaporation were obtained from the Department of Natural Resources and Watershed Management (DNRW) of the Kermanshah province. Our land cover map contained the classes of high-density natural forest (canopy cover > 75%), medium-density natural forest (canopy cover = 50–75%), low-density natural forest (canopy cover < 50%), planted forests, meadows, moderate-density grassland, and low-density grassland at 10-m resolution.

Reference information, overlaying process, and weights of the classified layers

We used previous wildfire statistics to generate a suitable source in our modeling and validation process. Therefore, all of the 74 wildfires (i.e., ground-truth data) which occurred during 2016–2020 were taken as reference data from DNRW. The information on previous wildfires was divided into two subsets. The first subset (70%) was used in the overlaying process, and the second subset (30%) was used to validate the final wildfire map. As a first step, we classified each wildfire factor (NDVI, elevation, slope, aspect, land cover, and evaporation) into four classes based on its range. Then, the first subset of the wildfire layer containing 30% of the data was overlaid on the classified factor layers. Based on the number of fires and burnt areas

in each class, the WR classes were determined. At the end of the process, four WR classes (very high, high, moderate, and low risk) were assigned to each factor. The GIS-based analyses were carried out in the QGIS (Ver. 3.16) interface, open-source GIS software.

Analytical hierarchy process (AHP)

The goal of the AHP technique is to select the best option based on different criteria through pairwise comparison (Lamat et al., 2021). The technique is also used for weighting criteria. Many studies have reported that AHP is a suitable tool for WR assessment (Akay & Şahin, 2019; Busico et al., 2019; Nikhil et al., 2021; Sivrikaya & Küçük, 2022). To determine the weight of each factor based on AHP, two general steps should be implemented: building a comparison matrix and calculating the weights of the factors. In the first step, all factors were compared with each other in terms of their importance. This step aims at determining which factors from each pair are more important and how many times more. To support the AHP, we generated a table based on all wildfire factors, which was used to conduct a pairwise comparison between all factors and to determine their importance based on findings of previous studies (Novkovic et al., 2021; Zhao et al., 2021) and discussions with local experts from the Natural Resources Bureau of Kermanshah province. Then, the weights of each factor were determined based on the pairwise compression. A pairwise comparison matrix was developed to compare all factors against each other based on their importance (equal, moderate, strong, very strong, and extremely strong). The weights for each factor were calculated by dividing the sum of each row with the total number of factors. Finally, to verify the generated weights, we used the Consistency Ratio (CR), which is calculated based on Eq. 2.

$$CR = \frac{CI}{RI} \tag{2}$$

where *CI* (Consistency Index) is the index characterizing the consistency of judgments across all pairwise comparisons and *RI* is the value of the random consistency index. Earlier studies reported that if the *CR* is lower than 0.1, then the set of judgments and weights are reliable (Nuthammachot & Stratoulias, 2021).

Validation of the wildfire risk (WR) model

The final product in the form of WR map was developed based on the linear combination of all six criteria (i.e., NDVI, elevation, slope, aspect, land cover, and evaporation). The weights of each criterion were assigned based on the estimations of the AHP. For the validation process, we overlaid the second subset of WR information (30%) with the resulted WR map. The accuracy of WR map was evaluated based on the overlapping of the areas contained in the modeled WR map classes (low, moderate, high, and very high) with the frequency of previous wildfire data.

Results

Potential wildfire factors, WR classes, and weights

The spatial distribution of the WR classes belonging to the 6 factors was mapped (Fig. 3; Table 1) across the study site, which was covered with vegetation (mainly with forests and grassland). Based on the overlaying results, low-density natural forests had a high level of WR probability (Fig. 3A). Areas with low elevation (Fig. 3B), and with the slope in the range of 40–60% (Fig. 3C), were found to have a high level of WR probability. Regarding the aspect classes, south-facing sides had a high WR probability (Fig. 3D). Land cover maps showed that a high-density natural forest class had the highest risk probability (Fig. 3E). In regard to the evaporation rate, WR increased in areas with an evaporation rate between 1539 and 2280 mm (Fig. 3F).

AHP-based WR model and validation

The comparison matrix and the weights of each factor are shown in Table 2. Based on our results, the elevation and aspect-based WRI layers had the highest and lowest weights, respectively. Also, the CR value of our model was 0.0798, which shows that the weights obtained from AHP are statistically reliable.

Based on the weights determined reliably by the means of the AHP, the WRI map was produced using Eq. 3.

$$\begin{aligned} WRI = {} & (23.7 \times Elevation) + (23.5 \times Evaporation) \\ & + (15.9 \times NDVI) + (14.1 \times Slope) \\ & + (12.1 \times LandCover) + (10.6 \times Aspect) \end{aligned} \tag{3}$$

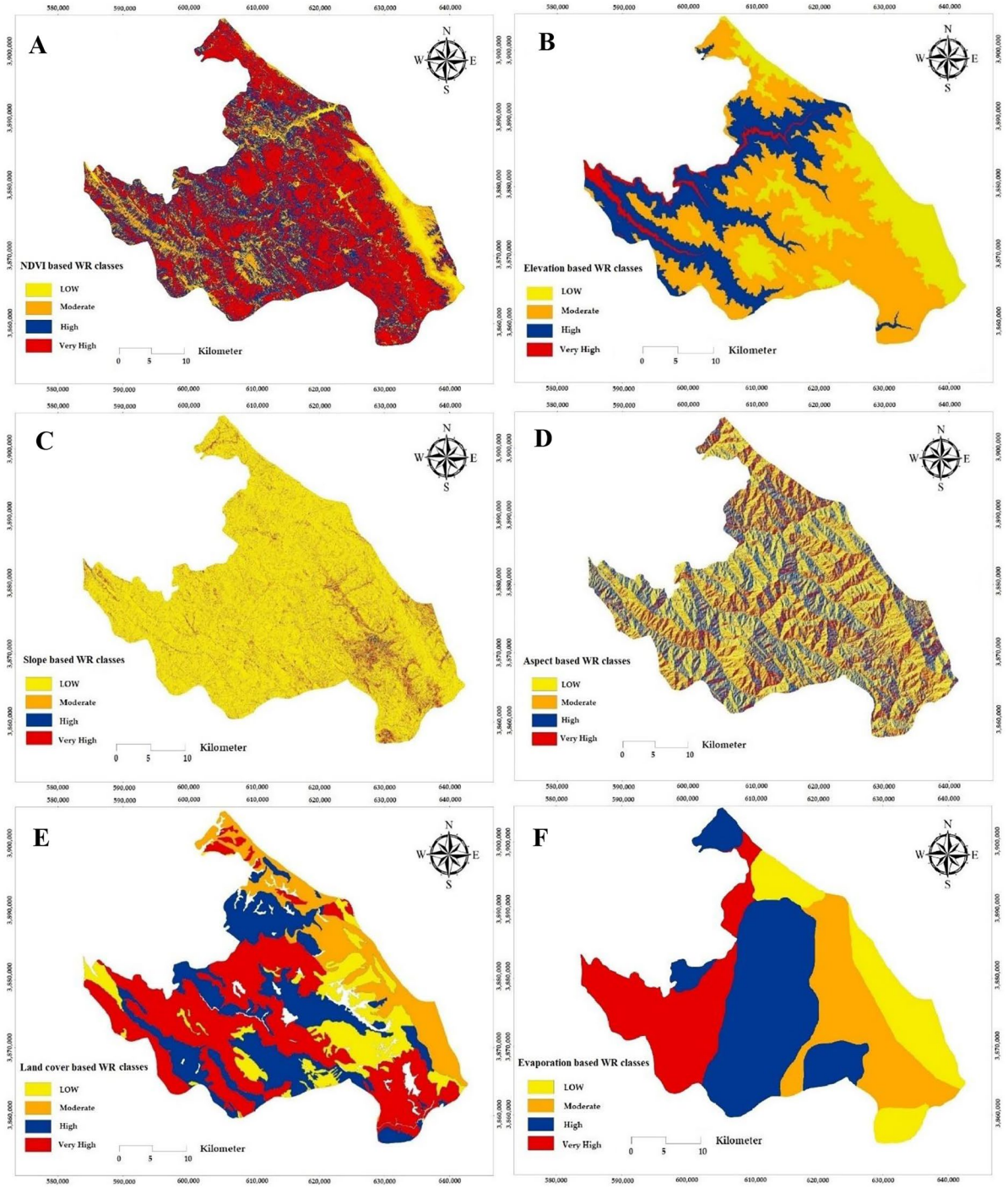

Fig. 3 Information layers used to develop the wildfire risk (WR) map in a study area. **A** NDVI; **B** elevation; **C** slope; **D** aspect; **E** land cover; and **F** evaporation

Table 1 Datasets used, factor values, weights, and wildfire risk (WR) class

Datasets	NDVI values	Weights	WR class
Remote sensing vegetation index	< 0.15	4	Very high
	0.15–0.3	3	High
	0.3–0.5	2	Moderate
	> 0.5	1	Low
	Elevation (m a.s.l)	Weights	WR class
Topographic features	< 1000	4	Very high
	1000–2000	3	High
	2000–3000	2	Moderate
	> 3000	1	Low
	Slope (%)	Weights	WR class
	40–60	4	Very high
	> 60	3	High
	20–40	2	Moderate
	< 20	1	Low
	Aspect	Weights	WR class
	South	4	Very high
	Southeast-southwest	3	High
	West–east-northeast	2	Moderate
	North-northwest-flat	1	Low
	Land cover	Weights	WR class
Land cover	High to medium density natural forests	4	Very high
	Low density natural forest-planted forest	3	High
	Meadows	2	Moderate
	Moderate to low density grasslands	1	Low
	Evaporation (mm yr^{-1})	Weights	WR class
Climate	1539–2280	4	Very high
	1352–1538	3	High
	1180–1351	2	Moderate
	640–1179	1	Low

The resulting WRI map is shown in Fig. 4. Our WRI map resulted in four zones, low, moderate, high, and very high WR, which have areas of 16,113; 25,044; 47,555; and 28,049 ha, respectively (Figs. 4 and 5). In more detail, 64.8% of our study site areas are located in high- and very high-risk zone classes (Fig. 5).

The results of the WRI map were validated by comparing them against the previous wildfire information (validation subset, 30% of the data). Based on the comparison results, we found that among the 52 fires which occurred during 2016–2020, a number of 38 data points were located in the high- and

Table 2 The comparison matrix of wildfire factors and their weights based on AHP

Datasets	Elevation	Slope	Aspect	Land cover	NDVI	Evaporation	Weight (%)
Elevation	1	2	2	3	2	1	23.8
Slope	0.5	1	1	2	1	0.5	14.1
Aspect	0.5	1	1	0.5	1	0.33	10.6
Land cover	0.33	0.5	2	1	1	0.5	12.1
NDVI	0.5	1	1	1	1	1	15.9
Evaporation	1	2	3	2	1	1	23.5

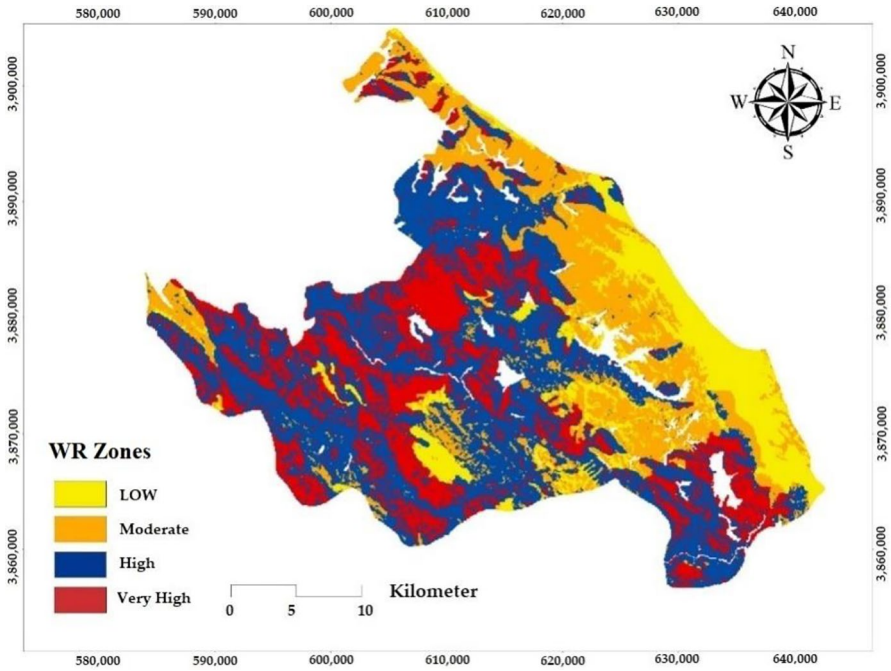

Fig. 4 Wildfire risk (WR) map of the study area (in white are the residential areas)

very high-risk zones of WR (Table 3). Therefore, the accuracy of the produced WRI map is of 87.57%.

Discussion

In the last decade, an accurate assessment of WR has become a challenge for natural resources managers. To increase the accuracy of WR assessments, the majority of previous studies considered factors such as topography, land use and land cover, and climatological and meteorological information. This study attempted to use all available datasets to produce a reliable WR model based on AHP- and GIS-based spatial analysis. Our results indicated that elevation is the most critical factor in WR modeling. The

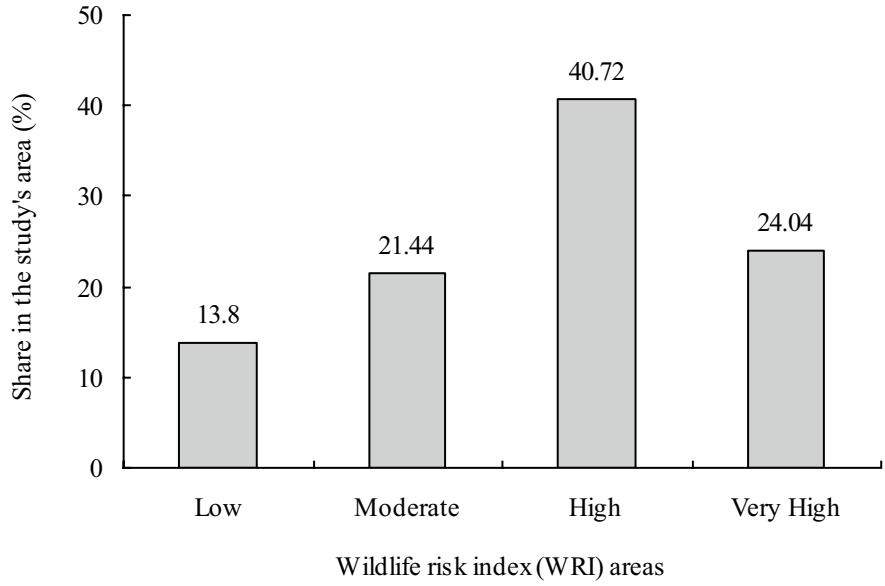

Fig. 5 Share of the wildfire risk index (WRI) areas in the study's area

Table 3 The results of overlaying previous wildfire data points with wildfire risk index (WRI) map ($n = 52$)

Classes	Point	Percentage
Low	4	7.69
Moderate	10	19.23
High	22	42.31
Very high	16	30.77

high weight of topographic factors was also reported in previous studies. For example, Zhao et al. (2021) allocated in their AHP-based WRI model the highest weight to topographic factors, including elevation, slope, aspect, and topographic wetness index. From a spatial point of view, our model's highest WR areas were located in the low-elevation areas of the study. Past research showed that fire tends to be less severe at higher elevations due to high rainfall (Sharma et al., 2012), high temperature (Bentekhici et al., 2020; Sivrikaya & Küçük, 2022), and the fact that fewer human activities occur in high elevation area (Yang et al., 2021). On the other hand, the low WR found by our model at high elevation gradients can be due to a lack of plant material and fuel, lower temperature, high humidity, low human accessibility, or a combination of these factors. In terms of aspect, the highest WR was observed on the southern sides, which can be explained by the incidence of more sunlight, making the fuel drier and more flammable. Accordingly, the aspect plays a significant role in WR susceptibility since it gives information about the terrain's relationship with sunlight and wind, thus greatly impacting fire ignition and spread (Arca et al., 2020; Jaiswal et al., 2002). The southern aspects receive more sunlight than the northern aspects, and, therefore, the southern aspects are more vulnerable to WR (Bentekhici et al., 2020; Lin & Rinaldi, 2009; Sari, 2021; Sivrikaya & Küçük, 2022). Past research suggested that steeper slopes, south-facing aspects, and lower elevations are also associated with a stronger likelihood of a WR (Prestemon et al., 2002; Bhandary & Muller, 2009). The influence of the slope factor was somewhat strong (14.1%). By overlaying the slope layer with previous wildfire data points, we found that slopes in the range of 40–60% experienced the highest number of previous wildfires, while on slope classes of less than 40% and more than 60%, the fire occurrence rate was lower. The NDVI factor had a weight of 15.9%. In similar studies, NDVI was always used to resemble vegetation attributes such as vegetation density and health status (Edwards et al., 2018; Giuseppi et al., 2021). Lower NDVI values in this study area increase WR, similar to the finding of Hong et al. (2018). Besides the NDVI, we also used a land cover map characterizing seven land cover classes: high-density natural forest, medium-density natural forest, low-density natural forest, planted forests, meadows, moderate-density grassland, and low-density grassland. Since our study site is mainly covered with forests and grasslands, more vegetation factors such as forest type, grassland type, forest canopy density, dead trees, and existing ground fuels could have been beneficial in increasing the assessment accuracy and producing a more accurate WRI map. Tomar et al. (2021) considered the forest type map in their process and allocated the highest weight to it. They reported that forest type is an essential factor because it provides sufficient information about the abundance of flammable materials. Other important factors in WR assessments that have always been of interest are climatological and meteorological factors. Tošić et al. (2019) used meteorological factors including temperature, precipitation, relative humidity, and wind speed and reported that these factors could produce a reasonable model for assessing WRs. In this study, we used the evaporation factor with a weight of 23.5% because it can also characterize other meteorological factors such as wind speed, temperature, and precipitation. The use of other factors such as evapotranspiration, vegetation types, tree health status, water content, socioeconomic factors, and long-term climatic conditions can improve the outputs of the WRI. Predictions on future climate change in the Zagros mountain vegetation zone (Dolatshahi et al., 2017) depict a trend of temperature increment at lower elevations, which will make thousands of hectares more vulnerable to wildfires.

Based on the WRI map, most of our study site is located in the high-risk zone (40.7% of the area), followed by a very high-risk zone (24.0% of the area), moderate-risk zone (21.4% of the area), and low-risk zone (13.8% of the area). As it can be seen, 64.7% of the study site is located in high- and very high-risk zones. Finding out which areas are susceptible to fire could help mitigate the problem and improve preventative actions. For instance, prescribed burning is one action that has been shown to be very effective in

fire-vulnerable areas (Edwards et al., 2021; Fernandes & Botelho, 2003). Therefore, it is necessary to develop and improve strategies for overcoming WR, such as allocating fire watchtowers and effective fire monitoring in areas with more fire events.

This study used AHP to compare factors and determine their weights. Although AHP is the most used model in WR assessment studies, some researchers used other approaches such as logistic regression (Milanović et al., 2021), neural networks (Zhang et al., 2021), random forest (Ma et al., 2020), and regression trees (Mohajane et al., 2021). The majority of these models need sufficient samples regarding previous wildfire information for model training and testing. Providing such information related to WR factors and samples is a methodological challenge. Integration of AHP and GIS, on the other hand, can output a reasonable model accuracy while producing an accurate WRI map based on a small set of labeled samples and available wildfire drivers. Accordingly, the accuracy of our model was found to be reasonable, accounting for approximately 88%. Therefore, AHP and GIS can be used as valuable tools for WR assessments. The high degree of agreement might be partially attributed to the AHP technique we have used for data analysis; similar studies have demonstrated a high accuracy when using AHP and GIS for WR assessment (Akbulak et al., 2018; Arca et al., 2020; Rasooli et al., 2018; Sari, 2021; Sivrikaya & Küçük, 2022).

Conclusion

The aim of this study was to evaluate the potential contribution of several wildfire drivers and to develop a local WRI map using GIS and AHP for the Zagros Mountains vegetation zone, which is a first-degree fire-sensitive region in the Mediterranean region of Iran. Our risk assessment process involved all available factors, including topographic factors, NDVI, land cover, and evaporation. Each factor was classified based on previous wildfire information, and, finally, WR classes were produced. In the AHP process, elevation and evaporation layers were considered the most critical factors. The accuracy of resulted WRI map was assessed using previous wildfire information and the efficiency of our methodology was confirmed. The final risk map shows that approximately 64.7% of the study area is located in the high- and very high-risk zones. WR maps are commonly used in many countries around the world, allowing for assessing factors that could lead to fires and providing useful information to the managers of natural resources, decision-makers, and firefighters.

Acknowledgements Vahid Nasiri's, Seyed Mohammad Moein Sadeghi's, and Azade Deljouei's research at the Transilvania University of Brasov, Romania, has been supported by the program entitled "Transilvania Fellowship for Postdoctoral Research/Young Researchers."

Author contribution Vahid Nasiri: conceptualization, methodology, software, data curation, investigations, validation, visualization, formal analysis, writing – original draft. Rasoul Bagherabadi: data curation, investigations. Seyed Mohammad Moein Sadeghi: conceptualization, methodology, software, formal analysis, writing – review and editing, supervision. Fardin Moradi: data curation, methodology, investigations, writing – original draft. Azade Deljouei: conceptualization, methodology, software, formal analysis, writing – review and editing, supervision. Stelian Alexandru Borz: writing – review and editing, supervision.

Data availability The data supporting the findings of this study are available from the first author, upon reasonable request.

Declarations

Conflict of interest The authors declare no competing interests.

References

Airey-Lauvaux, C., Pierce, A. D., Skinner, C. N., & Taylor, A. H. (2022). Changes in fire behavior caused by fire exclusion and fuel build-up vary with topography in California montane forests, USA. *Journal of Environmental Management, 304*, 114255. https://doi.org/10.1016/j.jenvman.2021.114255

Akay, A. E., & Şahin, H. (2019). Forest fire risk mapping by using GIS techniques and AHP method: A case study in Bodrum (Turkey). *European Journal of Forest Engineering*, *5*, 25–35. https://doi.org/10.33904/ejfe.579075

Akbulak, C., Tatlı, H., Aygün, G., & Sağlam, B. (2018). Forest fire risk analysis via integration of GIS, RS and AHP: The case of Çanakkale, Turkey. *Journal of Human Sciences, 15*, 2127–1243.

Amiri, M., & Pourghasemi, H. R. (2022). Mapping the NDVI and monitoring of its changes using Google Earth Engine and Sentinel-2 images. *Computers in Earth and Environmental Sciences*, pp. 127–136. https://doi.org/10.1016/B978-0-323-89861-4.00044-0

Arca, D., Hacısalihoğlu, M., & Kutoğlu, ŞH. (2020). Producing forest fire susceptibility map via multi-criteria decision analysis and frequency ratio methods. *Natural Hazards, 104*(1), 73–89. https://doi.org/10.1007/s11069-020-04158-7

Banerjee, P. (2021). MODIS-FIRMS and ground-truthing-based wildfire likelihood mapping of Sikkim Himalaya using machine learning algorithms. *Natural Hazards, 110*, 899–935. https://doi.org/10.1007/s11069-021-04973-6

Bashari, H., Naghipour, A. A., Khajeddin, S. J., Sangoony, H., & Tahmasebi, P. (2016). Risk of fire occurrence in arid and semi-arid ecosystems of Iran: An investigation using Bayesian belief networks. *Environmental Monitoring and Assessment, 188*, 1–15. https://doi.org/10.1007/s10661-016-5532-8

Bentekhici, N., Bellal, S. A., & Zegrar, A. (2020). Contribution of remote sensing and GIS to mapping the fire risk of Mediterranean forest case of the forest massif of Tlemcen (North-West Algeria). *Natural Hazards, 104*(1), 811–831. https://doi.org/10.1007/s11069-020-04191-6

Bhandary, U., & Muller, B. (2009). Land use planning and wildfire risk mitigation: An analysis of wildfire-burned subdivisions using high-resolution remote sensing imagery and GIS data. *Journal of Environmental Planning and Management, 52*(7), 939–955. https://doi.org/10.1080/09640560903181147

Bot, K., & Borges, J. G. (2022). A systematic review of applications of machine learning techniques for wildfire management decision support. *Inventions, 7*, 15. https://doi.org/10.3390/inventions7010015

Boucher, D., Gauthier, S., Thiffault, N., Marchand, W., Girardin, M., & Urli, M. (2020). How climate change might affect tree regeneration following fire at northern latitudes: A review. *New Forests, 51*, 543–571. https://doi.org/10.1007/s11056-019-09745-6

Busico, G., Giuditta, E., Kazakis, N., & Colombani, N. (2019). A hybrid GIS and AHP approach for modelling actual and future forest fire risk under climate change accounting water resources attenuation role. *Sustainability, 11*, 7166. https://doi.org/10.3390/su11247166

Carmo, M., Moreira, F., Casimiro, P., & Vaz, P. (2011). Land use and topography influences on wildfire occurrence in northern Portugal. *Landscape and Urban Planning, 100*(1–2), 169–176. https://doi.org/10.1016/j.landurbplan.2010.11.017

Carrasco, J., Acuna, M., Miranda, A., Alfaro, G., Pais, C., & Weintraub, A. (2021). Exploring the multidimensional effects of human activity and land cover on fire occurrence for territorial planning. *Journal of Environmental Management, 297*, 113428. https://doi.org/10.1016/j.jenvman.2021.113428

Coban, H., & Erdin, C. (2020). Forest fire risk assessment using GIS and AHP integration in Bucak forest enterprise, Turkey. *Applied Ecology and Environmental Research, 18*, 1567–1583. https://doi.org/10.15666/aeer/1801_15671583

Dolatshahi, A., Attarod, P., Zahedi, G., Sadeghi, S. M. M., & Bayramzadeh, V. (2017). Trends of meteorological parameters and reference evapotranspiration in the northern Zagros region. *Forest and Wood Products*, *70*, 251–260. https://doi.org/10.22059/jfwp.2017.62482

Edwards, A., Archer, R., De Bruyn, P., Evans, J., Lewis, B., & Vigilante, T. (2021). Transforming fire management in northern Australia through successful implementation of savanna burning emissions reductions projects. *Journal of Environmental Management, 290*, 112568. https://doi.org/10.1016/j.jenvman.2021.112568

Edwards, A. C., Russell-Smith, J., & Maier, S. W. (2018). A comparison and validation of satellite-derived fire severity mapping techniques in fire prone north Australian savannas: Extreme fires and tree stem mortality. *Remote Sensing of Environment, 206*, 287–299. https://doi.org/10.1016/j.rse.2017.12.038

Elia, M., D'Este, M., Ascoli, D., Giannico, V., Spano, G., Ganga, A., Colangelo, G., Lafortezza, R., & Sanesi, G. (2020). Estimating the probability of wildfire occurrence in Mediterranean landscapes using Artificial Neural Networks. *Environmental Impact Assessment Review, 85*, 106474. https://doi.org/10.1016/j.eiar.2020.106474

Emmett, K. D., Renwick, K. M., & Poulter, B. (2021). Adapting a dynamic vegetation model for regional biomass, plant biogeography, and fire modeling in the Greater Yellowstone Ecosystem: Evaluating LPJ-GUESS-LMfireCF. *Ecological Modelling, 440*, 109417. https://doi.org/10.1016/j.ecolmodel.2020.109417

Esfandeh, S., Danehkar, A., Salmanmahiny, A., Sadeghi, S. M. M., & Marcu, M. V. (2021). Climate change risk of urban growth and land use/land cover conversion: An in-depth review of the recent research in Iran. *Sustainability, 14*(1), 338. https://doi.org/10.3390/su14010338

Eslami, R., Azarnoush, M., Kialashki, A., & Kazemzadeh, F. (2021). GIS-based forest fire susceptibility assessment by random forest, artificial neural networrk and logistic regression methods. *Journal of Tropical Forest Science*, *33*, 173–184. https://doi.org/10.26525/jtfs2021.33.2.173

Fernandes, P. M., & Botelho, H. S. (2003). A review of prescribed burning effectiveness in fire hazard reduction. *International Journal of Wildland Fire, 12*, 117–128. https://doi.org/10.1071/WF02042

Gigović, L., Pourghasemi, H. R., Drobnjak, S., & Bai, S. (2019). Testing a new ensemble model based on SVM and random forest in forest fire susceptibility assessment and its mapping in Serbia's Tara National Park. *Forests, 10*, 408. https://doi.org/10.3390/f10050408

Giuseppi, A., Germanà, R., Fiorini, F., Delli Priscoli, F., & Pietrabissa, A. (2021). UAV patrolling for wildfire monitoring by a dynamic Voronoi Tessellation on satellite fata. *Drones, 5*(4), 130. https://doi.org/10.3390/drones5040130

Hardy, C. C. (2005). Wildland fire hazard and risk: Problems, definitions, and context. *Forest Ecology and Management, 211*, 73–82. https://doi.org/10.1016/j.foreco.2005.01.029

Hong, H., Tsangaratos, P., Ilia, I., Liu, J., Zhu, A. X., & Xu, C. (2018). Applying genetic algorithms to set the optimal combination of forest fire related variables and model forest fire susceptibility based on data mining models. The case of Dayu County, China. *Science of the Total Environment, 630*, 1044–1056. https://doi.org/10.1016/j.scitotenv.2018.02.278

Jaafari, A., Gholami, D. M., & Zenner, E. K. (2017). A Bayesian modeling of wildfire probability in the Zagros Mountains, Iran. *Ecological Informatics, 39*, 32–44. https://doi.org/10.1016/j.ecoinf.2017.03.003

Jaiswal, R. K., Mukherjee, S., Raju, K. D., & Saxena, R. (2002). Forest fire risk zone mapping from satellite imagery and GIS. *International Journal of Applied Earth Observation and Geoinformation, 4*(1), 1–10. https://doi.org/10.1016/S0303-2434(02)00006-5

Jiang, H., Wang, M., Hu, H., & Xu, J. (2021). Evaluating the performance of Sentinel-1A and Sentinel-2 in small

waterbody mapping over urban and mountainous regions. *Water, 13*(7), 945. https://doi.org/10.3390/w13070945

Jiang, T., Su, X., Singh, V. P., & Zhang, G. (2022). Spatio-temporal pattern of ecological droughts and their impacts on health of vegetation in Northwestern China. *Journal of Environmental Management, 305*, 114356. https://doi.org/10.1016/j.jenvman.2021.114356

Kim, S. J., Lim, C. -H., Kim, G. S., Lee, J., Geiger, T., & Rahmati, O. (2019). Multi-temporal analysis of forest fire probability using socio-economic and environmental variables. *Remote Sensing, 11*, 86. https://doi.org/10.3390/rs11010086

Lamat, R., Kumar, M., Kundu, A., & Lal, D. (2021). Forest fire risk mapping using analytical hierarchy process (AHP) and earth observation datasets: A case study in the mountainous terrain of Northeast India. *SN Applied Sciences, 3*, 1–15. https://doi.org/10.1007/s42452-021-04391-0

Lanaras, C., Bioucas-Dias, J., Galliani, S., Baltsavias, E., & Schindler, K. (2018). Super-resolution of Sentinel-2 images: Learning a globally applicable deep neural network. *ISPRS Journal of Photogrammetry and Remote Sensing, 146*, 305–319. https://doi.org/10.1016/j.isprsjprs.2018.09.018

Landi, M. A., Di Bella, C. M., Bravo, S. J., & Bellis, L. M. (2021). Structural resistance and functional resilience of the Chaco forest to wildland fires: An approach with MODIS time series. *Australian Ecology, 46*, 277–289. https://doi.org/10.1111/aec.12977

Li, X., Zhang, M., Zhang, S., Liu, J., Sun, S., & Hu, T. (2022). Simulating forest fire spread with cellular automation driven by a LSTM based speed model. *Fire, 5*, 13. https://doi.org/10.3390/fire5010013

Lin, J., & Rinaldi, S. (2009). A derivation of the statistical characteristics of forest fires. *Ecological Modelling, 220*(7), 898–903. https://doi.org/10.1016/j.ecolmodel.2009.01.011

Liu, C., Deng, T., Zhou, S., Yan, R., & Huang, L. (2021). Experimental investigation on fire risk assessment for typical interior wallpapers. *Fire Technology, 58*, 991–1009. https://doi.org/10.1007/s10694-021-01178-y

Ma, Q., Su, Y., Luo, L., Li, L., Kelly, M., & Guo, Q. (2018). Evaluating the uncertainty of Landsat-derived vegetation indices in quantifying forest fuel treatments using bi-temporal LiDAR data. *Ecological Indicators, 95*, 298–310. https://doi.org/10.1016/j.ecolind.2018.07.050

Ma, W., Feng, Z., Cheng, Z., Chen, S., & Wang, F. (2020). Identifying forest fire driving factors and related impacts in China using random forest algorithm. *Forests, 11*, 507. https://doi.org/10.3390/f11050507

Mallinis, G., Mitsopoulos, I., & Chrysafi, I. (2018). Evaluating and comparing Sentinel 2a and Landsat-8 operational land imager (OLI) spectral indices for estimating fire severity in a Mediterranean pine ecosystem of Greece. *GIScience & Remote Sensing, 55*, 1–18. https://doi.org/10.1080/15481603.2017.1354803

McGlynn, E., Li, S. F., Berger, M., Amend, M. L., & Harper, K. (2022). Addressing uncertainty and bias in land use, land use change, and forestry greenhouse gas inventories. *Climatic Change, 170*, 1–25. https://doi.org/10.1007/s10584-021-03254-2

Milanović, S., Marković, N., Pamučar, D., Gigović, L., Kostić, P., & Milanović, S. D. (2021). Forest fire probability mapping in eastern Serbia: Logistic regression versus random forest method. *Forests, 12*, 5. https://doi.org/10.3390/f12010005

Mitri, G., Jazi, M., & McWethy, D. (2015). Assessment of wildfire risk in Lebanon using geographic object-based image analysis. *Photogrammetric Engineering & Remote Sensing, 81*(6), 499–506. https://doi.org/10.14358/PERS.81.6.499

Mohajane, M., Costache, R., Karimi, F., Pham, Q. B., Essahlaoui, A., Nguyen, H., Laneve, G., & Oudija, F. (2021). Application of remote sensing and machine learning algorithms for forest fire mapping in a Mediterranean area. *Ecological Indicators, 129*, 107869. https://doi.org/10.1016/j.ecolind.2021.107869

Moradi, F., Darvishsefat, A. A., Pourrahmati, M. R., Deljouei, A., & Borz, S. A. (2022). Estimating aboveground biomass in fense Hyrcanian forests by the use of Sentinel-2 data. *Forests, 13*, 104. https://doi.org/10.3390/f13010104

Naderpour, M., Rizeei, H. M., & Ramezani, F. (2021). Forest fire risk prediction: A spatial deep neural network-based framework. *Remote Sensing, 13*, 2513. https://doi.org/10.3390/rs13132513

Nasiri, V., Deljouei, A., Moradi, F., Sadeghi, S. M. M., & Borz, S. A. (2022). Land use and land cover mapping using Sentinel-2, Landsat-8 satellite images, and Google Earth Engine: A comparison of two composition methods. *Remote Sensing, 14*(9), 1977. https://doi.org/10.3390/rs14091977

Nebot, À., & Mugica, F. (2021). Forest fire forecasting using fuzzy logic models. *Forests, 12*, 1005. https://doi.org/10.3390/f12081005

Nikhil, S., Danumah, J. H., Saha, S., Prasad, M. K., Rajaneesh, A., Mammen, P. C., Ajin, R. S., & Kuriakose, S. L. (2021). Application of GIS and AHP method in forest fire risk zone mapping: A study of the Parambikulam Tiger Reserve, Kerala, India. *Journal of Geovisualization and Spatial Analysis, 5*, 1–14. https://doi.org/10.1007/s41651-021-00082-x

Novkovic, I., Markovic, G. B., Lukic, D., Dragicevic, S., Milosevic, M., Djurdjic, S., Samardzic, I., Lezaic, T., & Tadic, M. (2021). GIS-based forest fire susceptibility zonation with IoT sensor network support, case study—Nature Park Golija, Serbia. *Sensors, 21*, 6520. https://doi.org/10.3390/s21196520

Nuthammachot, N., & Stratoulias, D. (2021). Multi-criteria decision analysis for forest fire risk assessment by coupling AHP and GIS: Method and case study. *Environment, Development and Sustainability, 23*, 17443–17458. https://doi.org/10.1007/s10668-021-01394-0

Nyamadzawo, G., Gwenzi, W., Kanda, A., Kundhlande, A., & Masona, C. (2013). Understanding the causes, socio-economic and environmental impacts, and management of veld fires in tropical Zimbabwe. *Fire Science Reviews, 2*, 1–13. https://doi.org/10.1186/2193-0414-2-2

Ozenen Kavlak, M., Cabuk, S. N., & Cetin, M. (2021). Development of forest fire risk map using geographical information systems and remote sensing capabilities: Ören case. *Environmental Science and Pollution Research, 28*, 33265–33291. https://doi.org/10.1007/s11356-021-13080-9

Pham, B. T., Jaafari, A., Avand, M., Al-Ansari, N., Du Dinh, T., Yen, H. P. H., Phong, T. V., Nguyen, D. H., Le, H. V., Mafi-Gholami, D., & Prakash, I. (2020). Performance evaluation of machine learning methods for forest fire modeling and prediction. *Symmetry, 12*, 1022. https://doi.org/10.3390/sym12061022

Prestemon, J. P., Pye, J. M., Butry, D. T., Holmes, T. P., & Mercer, D. E. (2002). Understanding broadscale wildfire risks in a human-dominated landscape. *Forest Science, 48*(4), 685–693. https://doi.org/10.1093/forestscience/48.4.685

Quintano, C., Fernández-Manso, A., & Fernández-Manso, O. (2018). Combination of Landsat and Sentinel-2 MSI data for initial assessing of burn severity. *International Journal of Applied Earth Observation and Geoinformation, 64*, 221–225. https://doi.org/10.1016/j.jag.2017.09.014

Rasooli, S., Bonyad, A., & Pir Bavaghar, M. (2018). Forest fire vulnerability map using remote sensing data, GIS and AHP analysis (case study: Zarivar Lake surrounding area). *Caspian Journal of Environmental Sciences*, *16*, 369–377. https://doi.org/10.22124/CJES.2018.3205

Roche, J. W., Goulden, M. L., & Bales, R. C. (2018). Estimating evapotranspiration change due to forest treatment and fire at the basin scale in the Sierra Nevada, California. *Ecohydrology, 11*, e1978. https://doi.org/10.1002/eco.1978

Ruffault, J., & Mouillot, F. (2017). Contribution of human and biophysical factors to the spatial distribution of forest fire ignitions and large wildfires in a French Mediterranean region. *International Journal of Wildland Fire, 26*(6), 498–508. https://doi.org/10.1071/WF16181

Saaty, T. L. (1988). What is the analytic hierarchy process? Mathematical models for decision support: Springer, pp. 109–121. https://doi.org/10.1007/978-3-642-83555-1_5

Santoro, A., Venturi, M., Piras, F., Fiore, B., Corrieri, F., & Agnoletti, M. (2021). Forest area changes in Cinque Terre National Park in the last 80 years. Consequences on landslides and forest fire risks. *Land, 10*, 293. https://doi.org/10.3390/land10030293

Sari, F. (2021). Forest fire susceptibility mapping via multi-criteria decision analysis techniques for Mugla, Turkey: A comparative analysis of VIKOR and TOPSIS. *Forest Ecology and Management, 480*, 118644. https://doi.org/10.1016/j.foreco.2020.118644

Satir, O., Berberoglu, S., & Donmez, C. (2016). Mapping regional forest fire probability using artificial neural network model in a Mediterranean forest ecosystem. *Geomatics, Natural Hazards and Risk, 7*, 1645–1658. https://doi.org/10.1080/19475705.2015.1084541

Sevinc, V., Kucuk, O., & Goltas, M. (2020). A Bayesian network model for prediction and analysis of possible forest fire causes. *Forest Ecology and Management, 457*, 117723. https://doi.org/10.1016/j.foreco.2019.117723

Sharma, L. K., Kanga, S., Nathawat, M. S., Sinha, S., & Pandey, P. C. (2012). Fuzzy AHP for forest fire risk modeling. *Disaster Prevention and Management: An International Journal., 21*, 160–171. https://doi.org/10.1108/09653561211219964

Si, L., Shu, L., Wang, M., Zhao, F., Chen, F., Li, W., & Li, W. (2022). Study on forest fire danger prediction in plateau mountainous forest area. *Natural Hazards Research*. https://doi.org/10.1016/j.nhres.2022.01.002

Sivrikaya, F., & Küçük, Ö. (2022). Modeling forest fire risk based on GIS-based analytical hierarchy process and statistical analysis in Mediterranean region. *Ecological Informatics, 68*, 101537. https://doi.org/10.1016/j.ecoinf.2021.101537

Sobhani, P., Esmaeilzadeh, H., Barghjelveh, S., Sadeghi, S. M. M., & Marcu, M. V. (2021). Habitat integrity in protected areas threatened by LULC changes and fragmentation: A case study in Tehran Province, Iran. *Land, 11*(1), 6. https://doi.org/10.3390/land11010006

Swan, M., Le Pla, M., Di Stefano, J., Pascoe, J., & Penman, T. D. (2021). Species distribution models for conservation planning in fire-prone landscapes. *Biodiversity and Conservation, 30*, 1119–1136. https://doi.org/10.1007/s10531-021-02136-4

Sweitzer, R., Furnas, B., Barrett, R., Purcell, K., & Thompson, C. (2016). Landscape fuel reduction, forest fire, and biophysical linkages to local habitat use and local persistence of fishers (*Pekania pennanti*) in Sierra Nevada mixed-conifer forests. *Forest Ecology and Management, 361*, 208–225. https://doi.org/10.1016/j.foreco.2015.11.026

Talucci, A. C., Forbath, E., Kropp, H., Alexander, H. D., DeMarco, J., Paulson, A. K., Zimov, N. S., Zimov, S., & Loranty, M. M. (2020). Evaluating post-fire vegetation recovery in Cajander Larch Forests in Northeastern Siberia using UAV derived vegetation indices. *Remote Sensing, 12*, 2970. https://doi.org/10.3390/rs12182970

Tiwari, A., Shoab, M., & Dixit, A. (2021). GIS-based forest fire susceptibility modeling in Pauri Garhwal, India: A comparative assessment of frequency ratio, analytic hierarchy process and fuzzy modeling techniques. *Natural Hazards, 105*, 1189–1230. https://doi.org/10.1007/s11069-020-04351-8

Tomar, J. S., Kranjčić, N., Đurin, B., Kanga, S., & Singh, S. K. (2021). Forest fire hazards vulnerability and risk assessment in Sirmaur district forest of Himachal Pradesh (India): A geospatial approach. *ISPRS International Journal of Geo-Information, 10*, 447. https://doi.org/10.3390/ijgi10070447

Tošić, I., Mladjan, D., Gavrilov, M. B., Živanović, S., Radaković, M. G., Putniković, S., Petrović, P., Mistridželović, I. K., & Marković, S. B. (2019). Potential influence of meteorological variables on forest fire risk in Serbia during the period 2000–2017. *Open Geosciences, 11*, 414–425. https://doi.org/10.1515/geo-2019-0033

Yang, X., Jin, X., & Zhou, Y. (2021). Wildfire risk assessment and zoning by integrating Maxent and GIS in Hunan Province, China. *Forests, 12*(10), 1299. https://doi.org/10.3390/f12101299

Ying, L., Han, J., Du, Y., & Shen, Z. (2018). Forest fire characteristics in China: Spatial patterns and determinants with thresholds. *Forest Ecology and Management, 424*, 345–354. https://doi.org/10.1016/j.foreco.2018.05.020

Zhang, G., Wang, M., & Liu, K. (2021). Deep neural networks for global wildfire susceptibility modelling. *Ecological Indicators, 127*, 107735. https://doi.org/10.1016/j.ecolind.2021.107735

Zhao, E., Liu, Y., Zhang, J., & Tian, Y. (2021). Forest fire smoke recognition based on anchor box adaptive generation method. *Electronics, 10*, 566. https://doi.org/10.3390/electronics10050566

Zhu, Q., Liu, Y., Jia, R., Hua, S., Shao, T., & Wang, B. (2018). A numerical simulation study on the impact of smoke aerosols from Russian forest fires on the air pollution over Asia. *Atmospheric Environment, 182*, 263–274. https://doi.org/10.1016/j.atmosenv.2018.03.052